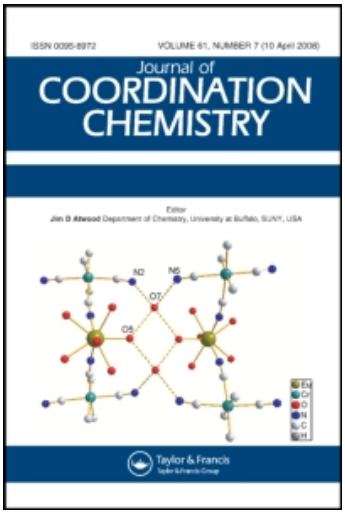

Journal of Coordination Chemistry
Publication details, including instructions for authors and subscription information:
http://www.informaworld.com/smpp/title~content=t713455674

How or not to calculate Ni(II) Werner-type complexes: evaluation of quantum chemical methods

Markus Walther[a]; Basam M. Alzubi[ab]; Ralph Puchta[ac]; Gerald Linti[d]; Roland Meier[a]; Rudi Van Eldik[a]
[a] Inorganic Chemistry, Department of Chemistry and Pharmacy, University of Erlangen-Nürnberg, D-91058 Erlangen, Germany [b] Department of Basic Science, Zarka University College, Al-Balqa Applied University, Zarka, Jordan [c] Computer Chemistry Center, Department of Chemistry and Pharmacy, University of Erlangen-Nürnberg, D-91052 Erlangen, Germany [d] Anorganisch-Chemisches Institut, D-69120 Heidelberg, Germany

First published on: 07 December 2010

To cite this Article Walther, Markus , Alzubi, Basam M. , Puchta, Ralph , Linti, Gerald , Meier, Roland and Van Eldik, Rudi(2011) 'How or not to calculate Ni(II) Werner-type complexes: evaluation of quantum chemical methods', Journal of Coordination Chemistry, 64: 1, 18 — 29, First published on: 07 December 2010 (iFirst)
To link to this Article: DOI: 10.1080/00958972.2010.538390
URL: http://dx.doi.org/10.1080/00958972.2010.538390

Journal of Coordination Chemistry
Vol. 64, No. 1, 10 January 2011, 18–29

Taylor & Francis
Taylor & Francis Group

How or not to calculate Ni(II) Werner-type complexes: evaluation of quantum chemical methods

MARKUS WALTHER†, BASAM M. ALZUBI†‡, RALPH PUCHTA†§, GERALD LINTI¶, ROLAND MEIER† and RUDI VAN ELDIK*†

†Inorganic Chemistry, Department of Chemistry and Pharmacy, University of Erlangen-Nürnberg, Egerlandstr. 1, D-91058 Erlangen, Germany
‡Department of Basic Science, Zarka University College, Al-Balqa Applied University, Zarka, Jordan
§Computer Chemistry Center, Department of Chemistry and Pharmacy, University of Erlangen-Nürnberg, Nägelsbachstr. 25, D-91052 Erlangen, Germany
¶Anorganisch-Chemisches Institut, Im Neuenheimer Feld 270, D-69120 Heidelberg, Germany

(*Received 25 August 2010; in final form 19 October 2010*)

Different semi-empirical methods (PM3(tm), AM1*, and PM6) that have parameters for Ni were evaluated for structural and energy calculations in comparison with DFT calculations (B3LYP/LANL2DZp) and X-ray structures. The reported crystal structure for $K_4[Ni(nta)_2)] \cdot 4H_2O$ (nta = nitrilotriacetate, monoclinic space group $P2_1/n$ (No. 14), $a = 10.024(2)$ Å, $b = 10.838(2)$ Å, $c = 10.631(2)$ Å, $\beta = 96.46(3)^\circ$, $V = 1147.6(4)$ Å^3, $Z = 2$) and the published X-ray structures for {(2S,3S)-1,4-dimethoxy-2,3-bis[(salicylidene)amino]-butane}nickel(II) and amine(salicylaldehyde thiosemicarbazonato)nickel(II), $[Ni(AST)NH_3]$, were used for structural evaluation. The performance of the methods was also tested for typical ligand-substitution reactions at Ni(II) centers involving displacement of NH_3 by L (L = PH_3, AsH_3, SbH_3, H_2O, H_2S, H_2Se, H_2Te) in $[Ni(NH_3)_3NH_3]^{2+}$ and $[Ni(AST)NH_3]$. Whereas PM6 performed well for the evaluation of the structural data, AM1* was found to reproduce the energies in an excellent way.

Keywords: Ni(II) complexes; Nitrilotriacetate; Semi-empirical methods; DFT

1. Introduction

Nickel is an important catalytic cofactor of enzymes found in bacteria, fungi, and plants [1–3]. These enzymes catalyze various reactions including both redox and non-redox chemistry [4] and allow organisms to adjust to different environmental situations. For example, nickel proteins play a significant role in the global carbon cycle [2, 5]. The biological chemistry of nickel, similar to that of other transition metals [6], is

*Corresponding author. Email: Rudi.vanEldik@chemie.uni-erlangen.de

ISSN 0095-8972 print/ISSN 1029-0389 online © 2011 Taylor & Francis
DOI: 10.1080/00958972.2010.538390

complicated because inappropriate amounts can be toxic and cause cell damage [7]. Thus, its distribution and uptake must be controlled in terms of environmental and biological processes.

Hetero-donor ligand–metal complexes have received considerable attention during recent years. By way of example, histidine-tagged proteins were found to bind specifically to Ni–nta (nta = nitrilotriacetate) moieties to form a His–Ni–nta ternary complex. This complex is used for purification purposes, surface functionalization, and bidimensional crystallization through Ni–nta functionalized lipids [8, 9]. Homo-donor ligand–metal complexes, such as metal–bis(carboxylate) [10], metal–bis(phosphonate) [11], and metal–bis(terpyridine) [12], have also been used to generate supramolecular systems with unique structures and novel optical, electric, or magnetic properties. Ni(II) complexes with salen (salen = ethylenediamine-*N*,*N*′-bis(salicylaldimine)) [13] are well suited for covalent modification since the $Ni^{III/II}$ couple often lies near the redox potential of the ligand, at *ca* 1 V *versus* SCE. In addition, the irreversibility of the cyclic voltammograms of most Ni(II)–salen type complexes suggests that one-electron oxidation is ligand based and leads to phenolic radicals [14]. It is likely that ligand radical intermediates, when bound to DNA, may interact with reactive groups on nucleobases to form covalent bonds [15].

Nickel is known for its rich coordination chemistry [16] and an extensive organometallic chemistry [17–19]. Oxidation states of Ni range from −1 to +4, but the +2 state is by far the most common. In its complexes the d^8 Ni^{2+} ion is usually four-, five-, or six-coordinate and exhibits a range of coordination geometries that include paramagnetic tetrahedral and octahedral complexes, and diamagnetic square planar complexes [17]. Rulíšek and Havlas [20] studied $[Ni(H_2O)_5L]^{2+}$ complexes (L = H_2O, CH_3OH, CH_3SH, and NH_3) applying the B3LYP hybrid functional in conjunction with a variety of all electron basis sets, and demonstrated that the B3LYP functional in combination with a 6-311+G(d,p) basis set is a computationally efficient and reliable method. Similar results were obtained by Varadwaj *et al*. [21] in their studies on $[Ni(NH_3)_n(H_2O)_{6-n}]^{2+}$, $0 \le n \le 6$ using UX3LYP/6-311++G(d,p). Deeth and coworkers [22] studied the ability of DFT methods to reproduce observed crystallographic bond lengths of transition metal compounds of the type $[MA_nB_{m-n}]$ (M: e.g., Ni(II); A, B: a variety of N-, O-, P-, and C-donor ligands, Cl^-, CO). They showed that the gas-phase calculations systematically overestimated the metal–ligand bond length and that the incorporation of environmental effects by including a solvation model significantly improved the agreement between the observed and computed structures.

Nickel is inherently difficult to compute by semi-empirical methods as the classical model uses only s and p orbital basis sets, whereas d orbitals are important for the description of transition metals. In the present study, we focus on a comparison between the results of semi-empirical methods including parameters for Ni, like PM3(tm) [23], AM1* [24], and PM6 [25], and hybrid-DFT (B3LYP) calculations including effective core potentials (LANL2DZp) that can be applied to larger systems and to atoms where the inclusion of relativistic effects is essential. The computed structures were compared to experimental X-ray data for three different complexes. In addition, the reaction energies for a series of related ligand-substitution reactions of NH_3 in $[Ni(NH_3)_3NH_3]^{2+}$ and $[Ni(AST)NH_3]$ by PH_3, AsH_3, SbH_3, H_2O, H_2S, H_2Se, and H_2Te were calculated using the mentioned computational methods.

2. Experimental and computational chemistry

2.1. *Instruments and materials*

IR spectra were recorded on a Varian Excalibur FTS-3500 FT-IR-spectrometer in KBr pellets.

2.2. *Preparation of $K_4[Ni(nta)_2)] \cdot 4H_2O$ (1)*

Nitrilotriacetic acid (H_3nta) (5.82 g, 0.02 mol) and 2.70 g (0.01 mol) $Ni(NO_3)_2 \cdot 6H_2O$ were stirred in 20 mL water on a stirring plate with heating. An amount of 6.01 g (0.06 mol) of $KHCO_3$ was gently added over a period of 15 min to the slurry, the color of which changes from initially green to clear bluish upon heating and addition of bicarbonate. The resulting clear solution was heated for an hour at 80°C. After cooling to room temperature, ethanol was added until the first turbidity appeared. The solution was then placed in a refrigerator (at 5°C). After several days, blue crystals suitable for X-ray crystallography were formed and removed by suction. Yield: 5.2 g (78%). Anal. Calcd for $C_{12}H_{20}K_4N_2NiO_{16}$ (663.4 g mol^{-1}) (%): C, 21.72; H, 3.04; N, 4.22. Found (%): C, 21.50; H, 3.20; N, 4.15. Main IR absorption bands observed for **1** (KBr pellet/cm^{-1}) in the region between 1800 and 1000 cm^{-1} are: 1693, 1617 (br), 1393 (vs), 1305 (vs), 1216 (s), 1129 (s), 1108 (s).

2.3. *Crystal structure determination*

Suitable crystals of **1** were mounted with a perfluorated polyether oil on the tip of a glass fiber and cooled immediately on the goniometer head. Data collection was performed on a STOE IPDS I diffractometer with Mo-Kα radiation ($\lambda = 0.71073$ Å). Structures were solved and refined with the Bruker AXS *SHELXTL 5.1* program package. Refinement was in full matrix against F^2. All hydrogens were included as riding models with fixed isotropic U values in the final refinement. For further data see table 1.

2.4. *Quantum chemical methods*

Semi-empirical calculations were performed for PM3(tm) [23] with Titan [26], for AM1* [24] and PM6 [25] with VAMP 10.0 [27]. To compare semi-empirical and DFT results, B3LYP/LANL2DZp hybrid density functional calculations, that is, with pseudo-potentials on the heavy elements and the valence basis set augmented with polarization functions, were performed [28, 29]. Structures were characterized as minima, transition structures, etc., by computation of vibrational frequencies. Relative energies were corrected for zero point vibrational energy. Additional calculations applying the CPCM [30] solvent model as implemented in GAUSSIAN 09 were done with GAUSSIAN 09 [31], while for all other calculations the GAUSSIAN 03 suite of programs were used [32].

Table 1. Crystal data for the structure determination for $K_4[Ni(nta)_2)] \cdot 4H_2O$ (**1**).

	1
Empirical formula	$C_{12}H_{20}K_4N_2NiO_{16}$
Formula weight	663.39
Temperature (K)	200(2)
Wavelength, λ (Å)	0.71073
Crystal color, form	Blue, block
Crystal system	Monoclinic
Space group	$P2_1/n$ (No. 14)
Unit cell dimensions (Å, °)	
a	10.024(2)
b	10.838(2)
c	10.631(2)
α	90
β	96.46(3)
γ	90
Volume (A^3), Z	1147.6(4), 2
Crystal size (mm^3)	$0.30 \times 0.30 \times 0.20$
Calculated density ($g\,cm^{-3}$)	1.920
Absorption coefficient (mm^{-1})	1.652
θ range for data collection (°)	2.69–28.20
Observed data ($I > 2\sigma(I)$)	2407
Data/parameters	2785/178
R_1[a]	0.0227
wR_2[a]	0.0597
Goodness-of-fit on F^2	1.03

[a] $R_1 = \Sigma||F_o| - |F_c||/\Sigma|F_o|$.
[b] $wR_2 = [\Sigma[w(F_o^2 - F_c^2)^2]/\Sigma(F_o)^2]]^{1/2}$; $w = 1/[\sigma^2(F_o^2) + (0.0425P)^2]$, where $P = (F_o^2 + 2F_c^2)/3$.

3. Results and discussion

Three examples were selected to test the quality of the differently calculated structures, one from our ongoing work on $K_4[Ni(nta)_2)] \cdot 4H_2O$ (**1**), nta = nitrilotriacetate, and two from the literature, namely, {(2S,3S)-1,4-dimethoxy-2,3-bis[(salicylidene)amino]-butane}nickel(II) (**2**) [13] and amine(salicylaldehyde thiosemicarbazonato)nickel(II) (**3**) [Ni(AST)NH_3] [33]. For all three complexes the X-ray structures are known and their moderate size allowed theoretical calculations with the different quantum chemical methods mentioned above.

3.1. *Description of the crystal structure of 1*

The structure of $K_4[Ni(nta)_2)] \cdot 4H_2O$ (**1**) was solved in the monoclinic space group $P2_1/n$ with the asymmetric unit consisting of one-half of the molecular anion $[Ni(nta)_2]^{4-}$ (cf figure 1) and two crystallographic independent potassium cations (for details, see table 1). The full anion is generated by the symmetry operation of an inversion center. This sort of asymmetric unit was found in all Ni^{II} bis-nta structures studied so far [34–36] as well as in closely related Ni^{II} bis-chelate complexes [37–39]. An ORTEP diagram of **1** is shown in figure 1. Selected bond lengths and angles for **1** are listed in table 2. Ni–L distances and L–Ni–L′ angles compare well with those found in two closely related complexes [34–39].

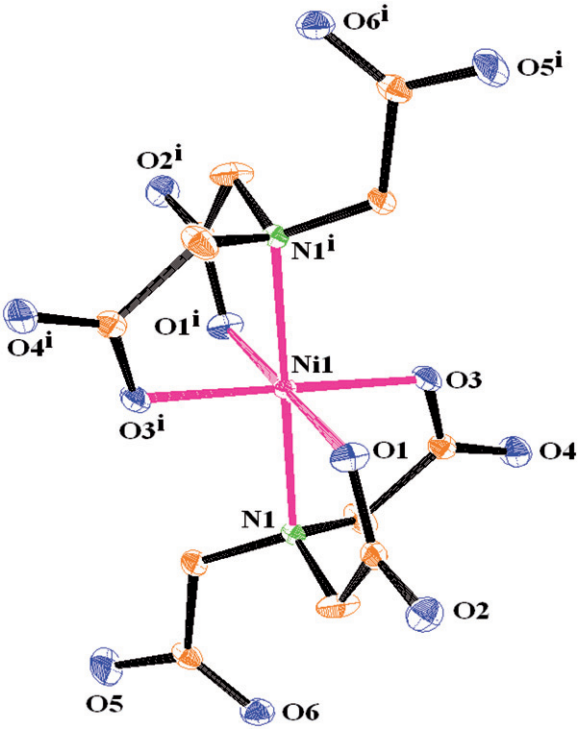

Figure 1. ORTEP diagram of $[Ni(nta)_2]^{4-}$ as found in **1** with atom numbering scheme (thermal ellipsoids are drawn at the 50% probability level). The symbol i indicates symmetry operation $(-x, -y, -z)$ at an inversion center.

Table 2. Selected bond lengths (Å) and angles (deg) for **1**.

Ni1–O1	2.0239(10)
Ni1–O3	2.0791(12)
Ni1–N1	2.1029(12)
O1–Ni1–O3	89.24(4)
O1–Ni1–O3^{i}	90.18(4)
O1–Ni1–N1	84.18(5)
O1–Ni1–N1^{i}	95.82(4)
O3–Ni1–N1	81.34(5)
O3–Ni1–N1^{i}	98.66(4)

Symmetry code ^{i}: $-x, -y+2, -z+1$.

3.2. *Calculated structures*

The first step to check the performance of a quantum chemical method is to compare the calculated structures with experimental data. A non-trivial case for all kinds of calculations is $[Ni(nta)_2]^{4-}$ as it is a tetra anion and shows two potentially freely dangling glycinate moieties. In the crystal structure of **1** the four negative charges are compensated by K^+. These K^+ ions are bound to the deprotonated glycinate COO^- groups, and additional water ligands contribute to the linkage of the $[Ni(nta)_2]^{4-}$ units. These complicated structural motives and the resulting environmental effects cannot be

Table 3. Comparison of structural data acquired by different methods for $[Ni(nta)_2]^{4-}$ (C_i) and $[Ni(ntaH)_2]^{2-}$ (C_i).

$Ni(nta)_2]^{4-}$	PM3(tm) [40]	AM1*	PM6	LANL2DZp	CPCM [41]	Crystal structure $[Ni(nta)_2]^{4-}$
Ni1–O1 (Å)	–	1.99	2.08	2.13	2.10	2.02
Ni1–O3 (Å)	–	2.00	2.06	2.08	2.06	2.08
Ni1–N1 (Å)	–	2.22	1.97	2.21	2.15	2.10
O1–Ni1–O3 (°)	–	90.5	92.8	90.8	89.6	89.2
O1–Ni1–O3^{i} (°)	–	89.6	87.2	89.2	90.4	90.2
O1–Ni1–N1 (°)	–	85.2	84.8	79.2	81.2	84.2
O1–Ni1–N1^{i} (°)	–	94.8	95.3	100.8	98.8	95.8
O3–Ni1–N1 (°)	–	84.7	86.9	82.7	83.9	81.3
O3–Ni1–N1^{i} (°)	–	95.2	93.2	97.3	96.1	98.7

$[Ni(ntaH)_2]^{2-}$	PM3(tm)	AM1*	PM6	LANL2DZp [42]	CPCM	$[Ni(ntaH)_2]^{2-}$ [36]	Crystal structure $[Ni(nta)_2]^{4-}$
Ni1–O1 (Å)	1.86	1.99	2.04	2.08	2.06	2.03	2.02
Ni1–O3 (Å)	1.85	1.98	2.02	2.06	2.06	2.05	2.08
Ni1–N1 (Å)	1.91	2.20	1.95	2.13	2.15	2.12	2.10
O1–Ni1–O3 (°)	87.6	90.4	89.1	89.1	88.2	89.7	89.2
O1–Ni1–O3^{i} (°)	92.4	89.6	90.9	90.9	91.9	90.3	90.2
O1–Ni1–N1 (°)	94.0	84.9	86.1	82.6	83.7	82.7	84.2
O1–Ni1–N1^{i} (°)	86.0	95.1	93.9	97.4	96.3	97.3	95.8
O3–Ni1–N1 (°)	93.0	85.5	88.0	82.9	83.4	81.0	81.3
O3–Ni1–N1^{i} (°)	87.0	94.5	92.1	95.1	96.6	99.0	98.7

LANL2DZp: B3LYP/LANL2DZp, CPCM: B3LYP(CPCM)/LANL2DZp, PM3(tm): PM3(tm), AM1*: AM1*, PM6: PM6.
^{i} denotes "center of symmetry".

easily modeled in quantum chemical calculations. In order to consider neighboring effects in these calculations, an implicit solvent model can be applied. An alternative way to obtain a working model is to reduce the negative charges on the $[Ni(nta)_2]^{4-}$ entity to two by protonation of the two non-coordinating COO^- groups, leading to the experimentally known complex $[Ni(ntaH)_2]^2$ [36]. This is only a rough approximation for the counter ion effects (table 3).

An uncharged system with Ni–N and Ni–O interactions is **2** (figure 2), a typical salen complex originally studied to learn more about the stereochemistry of asymmetric epoxidation reactions [13]. The results are summarized in table 4.

To further include Ni–S interactions, **3** (figure 3) was added to the test series since it can also serve as a system for the energy comparison of ligand-exchange reactions. The results are summarized in table 5.

As expected, DFT calculations show the best agreement with the X-ray data and can be improved by inclusion of an implicit solvent model as already reported by Deeth *et al.* [22]. The effect on our calculations was not so large that we would consider the application of such a solvent model to be mandatory. Whereas the structures of **2** and **3** can be reproduced without noteworthy differences by DFT and PM6, followed to some lower extent by AM1* and PM3(tm), the differences for the structure of **1** are considerably larger, independent of the selected method, but still acceptable. The structural differences between $[Ni(ntaH)_2]^{2-}$ and $[Ni(nta)_2]^{4-}$ are rather small based on the X-ray data, allowing the use of the protonated species $[Ni(ntaH)_2]^{2-}$ as a crude working model for the calculation of $[Ni(nta)_2]^{4-}$ influenced by the counter ions in the

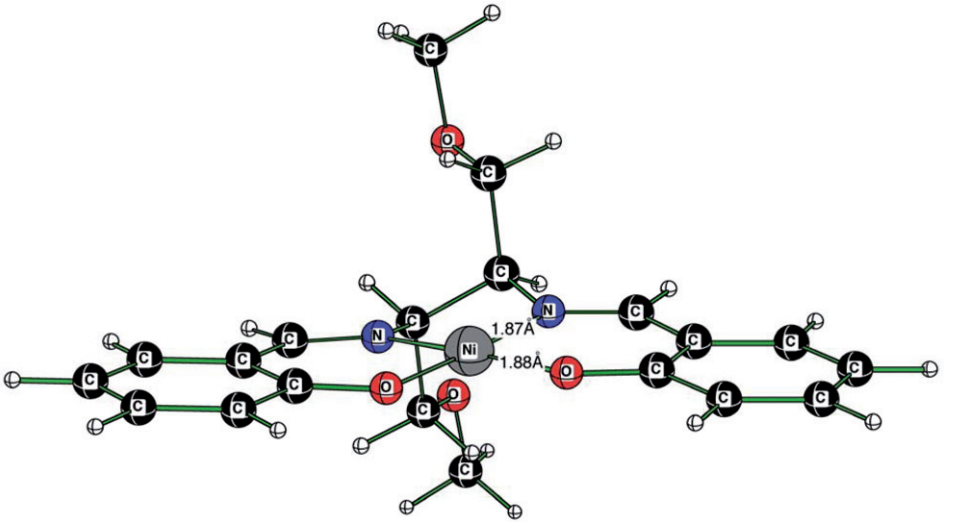

Figure 2. Calculated (B3LYP(CPCM)/LANL2DZp) structure of **2**.

Table 4. Comparison of structural data acquired by different methods for **2**.

Complex **2**	PM3(tm)	AM1*	PM6	LANL2DZp	CPCM	X-ray [13]
Mn–O (Å)	1.82	1.88	1.85	1.87	1.88	1.85/1.84
Mn–N (Å)	1.83	2.05	1.87	1.88	1.87	1.86
O–Mn–O (°)	72.6	85.0	77.5	86.3	85.9	85.4
O–Mn–N (°)	98.4	96.1	97.5	94.1	94.2	94.3/94.7
N–Mn (°)	90.6	83.0	87.5	85.7	85.7	86.1

LANL2DZp: B3LYP/LANL2DZp, CPCM: B3LYP(CPCM)/LANL2DZp, PM3(tm): PM3(tm), AM1*: AM1*, PM6: PM6.

solid state. This is confirmed by our calculations since the quantum chemical results for $[Ni(ntaH)_2]^{2-}$ are closer to the X-ray data for $[Ni(nta)_2]^{4-}$ than the calculated data for the uninfluenced $[Ni(nta)_2]^{4-}$ in the so-called gas phase. Addition of the CPCM solvent model to the DFT calculations only leads to a slight improvement of the results. This behavior clearly shows the importance of the counter ions and neighboring effects in such systems that could not be properly considered in all the different calculations performed for **1**. In terms of semi-empirical methods, AM1* is, in the case of $[Ni(nta)_2]^{4-}$, closer to the experimental values than PM6, independent of whether $[Ni(ntaH)_2]^{2-}$ or $[Ni(nta)_2]^{4-}$ is calculated.

3.3. *Calculated ligand-substitution reactions*

The applicability of the employed quantum chemical methods was further tested for two related ligand-substitution reactions of square-planar Ni(II) complexes, namely, $[Ni(NH_3)_3NH_3]^{2+}$ and derivatives of $[Ni(AST)NH_3]$ (figure 3) [33]. In these reactions NH_3 was substituted by L = PH_3, AsH_3, SbH_3, OH_2, SH_2, SeH_2, and TeH_2, and the

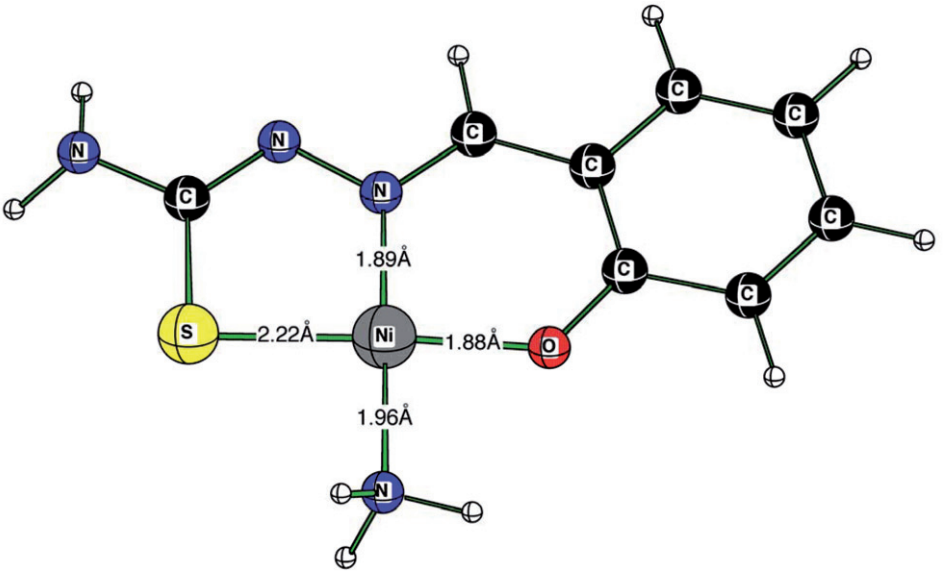

Figure 3. Calculated (B3LYP(CPCM)/LANL2DZp) structure of **3**.

Table 5. Comparison of structural data acquired by different methods for **3**.

Complex **3**	PM3(tm)	AM1*	PM6	LANL2DZp	CPCM	X-ray [33]
Ni–NH_3 (Å)	1.88	2.09	1.95	1.97	1.95	1.92
Ni–S (Å)	2.23	2.17	2.19	2.21	12.22	2.14
Ni–N (Å)	1.84	2.08	1.85	1.88	1.89	1.86
Ni–O (Å)	1.84	1.89	1.87	1.87	1.88	1.84
NH_3–Ni–S (°)	88.9	93.9	91.2	92.1	91.7	91.7
NH_3–Ni–O (°)	83.4	83.8	79.7	96.1	85.2	85.4
O–Ni–N (°)	96.0	94.8	99.4	96.2	95.7	95.7
S–Ni–N (°)	91.6	88.0	89.7	92.2	87.4	87.6

LANL2DZp: B3LYP/LANL2DZp, CPCM: B3LYP(CPCM)/LANL2DZp, PM3(tm): PM3(tm), AM1*: AM1*, PM6: PM6.

reaction energies were evaluated for reactions (1) and (2), respectively. The results are summarized in table 6.

$$[Ni(NH_3)_3NH_3]^{2+} + L \rightarrow [Ni(NH_3)_3L]^{2+} + NH_3 \quad (1)$$

$$[Ni(AST)NH_3]^{2+} + L \rightarrow [Ni(AST)L]^{2+} + NH_3 \quad (2)$$

As seen from table 6, AM1* shows the best performance compared to B3LYP/LANL2DZp calculations for the energy change during the ligand-substitution reactions. Unfortunately, there are no parameters for Se, Te, As, and Sb in AM1*. To obtain a more quantitative evaluation, the variances and averages of the relative differences were calculated (table 7). For AM1* the variance was found to be five times smaller than for PM6, and even an order of magnitude smaller than for PM3(tm).

Table 6. Comparison of calculated reaction energies for ligand substitution on $[Ni(NH_3)_3NH_3]^{2+}$ and $[Ni(AST)NH_3]^{2+}$ (**3**).

ΔE (kcal mol^{-1})	PM3(tm)	AM1*	PM6	LANL2DZp
$[Ni(NH_3)_3NH_3]^{2+}$	0	0	0	0
$[Ni(NH_3)_3OH_2]^{2+}$	29.62	−31.81	−23.34	−11.92
$[Ni(NH_3)_3SH_2]^{2+}$	−19.69	−20.81	−10.49	−21.10
$[Ni(NH_3)_3SeH_2]^{2+}$	−24.58	[48]	[43]	−19.03
$[Ni(NH_3)_3TeH_2]^{2+}$	[44]	[48]	[45]	−15.57
$[Ni(NH_3)_3PH_3]^{2+}$	−13.01	−52.52	49.59	−13.07
$[Ni(NH_3)_3AsH_3]^{2+}$	−95.44	[48]	[46]	−16.23
$[Ni(NH_3)_3SbH_3]^{2+}$	−141.42	[48]	[47]	−18.05
$[Ni(AST)NH_3]$ (**3**)	0	0	0	0
$[Ni(AST)OH_2]$	35.24	−24.85	−17.95	−8.83
$[Ni(AST)SH_2]$	−19.63	−18.18	−8.21	−16.52
$[Ni(AST)SeH_2]$	−25.59	[48]	[43]	−16.48
$[Ni(AST)TeH_2]$	[49]	[48]	[45]	−15.90
$[Ni(AST)PH_3]$	−24.88	−39.43	46.34	−12.76

LANL2DZp: B3LYP/LANL2DZp, PM3(tm): PM3(tm), AM1*: AM1*, PM6: PM6.

Table 7. Variance and average of relative differences of calculated reaction energies for ligand exchange at $[Ni(NH_3)_3NH_3]^{2+}$ and $[Ni(AST)NH_3]^{2+}$ (**3**).

$[Ni(NH_3)_3NH_3]^{2+}$			
Variance of relative differences	PM3(tm)	AM1*	PM6
Distances	0.00070	0.00162	0.00041
Angles	0.00542	0.00448	0.00702
Energies	12.50	1.45	5.43
$[Ni(AST)NH_3]^{2+}$			
Average of relative differences	PM3(tm)	AM1*	PM6
Distances	−0.02599	0.04461	−0.00457
Angles	−0.01754	−0.16255	−0.02069
Energies	1.24	1.08	−1.05

PM3(tm): PM3(tm), AM1*: AM1*, PM6: PM6.

The average of the relative differences is also the smallest for AM1*. When looking at PM3(tm), the positive average and large variance show that PM3(tm) consistently overestimates the energies, while the negative average values for PM6 show that this method underestimates the energies, but not to the degree as large as the overestimation of PM3(tm).

As shown before, the B3LYP/LANL2DZp structures are in good agreement with the experimental X-ray values [29d, e, g]. To obtain a more quantitative and uninfluenced neighboring-effect picture of the performance of the tested semi-empirical structures, we also calculated the variance and average difference for the structural data of the selected test set compared to the B3LYP/LANL2DZp structures (for structural data see Supplementary material). In terms of interatomic distances, PM6 shows the lowest variance, which indicates that the results are closest to B3LYP/LANL2DZp, whereas for PM3(tm) the variance is almost twice as high, and the five times higher absolute value and negative sign of the average indicate a consistent underestimation. AM1* has the highest variance and a large absolute value for the average with a positive sign, showing that this method is consistently overestimating interatomic distances for this small test set.

The picture is not quite as clear when looking at the predicted angles. All three methods show variances that are close to each other, and all three methods show large negative averages, meaning that all three methods underestimate the angles. However, the average of the relative differences for AM1* is one order of magnitude larger in absolute terms, which means that AM1* has the same statistical probability of getting the angles right, but shows larger differences than the values predicted by B3LYP/LANL2DZp.

4. Conclusions

Critical evaluation of results is mandatory irrespective of the applied method, in computational chemistry as well as in experimental science. No method can be regarded as a black box and considered to be always perfectly reliable, in particular when methods are selected on the basis of a compromise between accuracy and performance. These potential shortcomings dictate an individual and careful evaluation, to determine the optimal method for each problem and to reach an acceptable level of confidence, prior to the production of data. Evaluation may uncover existing systematic errors which subsequently can be eliminated from the results. Evaluation is in the highest interest of the user if unpublished methods are to be applied, due to the unavailability of original reference data. Analogously, this also is true for the exploration of systems new to a particular method.

Whereas our DFT calculations ran without significant problems, calculations performed with the semi-empirical methods warrant a closer look. We clearly favor AM1* for the prediction of energies, whereas PM3(tm) had the worst performance for energies. Our analysis showed superior performance of AM1* in that area. For distances and angles, or more general molecular geometry, PM6 appears to show the best performance, although the differences here are not as clear cut as they are for the prediction of energies.

Supplementary material

Structural data were deposited at the CCDC under Ref. No. CCDC 790316.

Acknowledgments

The authors gratefully acknowledge financial support from the Deutsche Forschungsgemeinschaft. We would like to thank Prof. Tim Clark for hosting this work at the CCC and the Regionales Rechenzentrum Erlangen (RRZE) for a generous allotment of computer time. B.M. Alzubi thanks Al-Balqa Applied University for their support.

References

[1] (a) J. Gerendás, J.C. Polacco, S.K. Freyermuth, B. Sattelmacher. *J. Plant Nutr. Soil Sci.*, **162**, 241 (1999); (b) S.B. Mulrooney, R.P. Hausinger. *FEMS Microbiol. Rev.*, **27**, 239 (2003); (c) B.T.A. Muyssen, K.V. Brix, D.K. DeForest, C.R. Janssen. *Environ. Rev.*, **12**, 113 (2004).
[2] S.W. Ragsdale. *J. Inorg. Biochem.*, **101**, 1657 (2007).
[3] (a) M. Maroney. *Curr. Opin. Chem. Biol.*, **3**, 188 (1999); (b) R.K. Watt, P.W. Ludden. *Cell. Mol. Life Sci.*, **56**, 604 (1999); (c) Y. Li, D.B. Zamble. *Chem. Rev.*, **109**, 4617 (2009).
[4] S.W. Ragsdale. *J. Biol. Chem.*, **284**, 18571 (2009).
[5] (a) U. Ermler, W. Grabarse, S. Shima, M. Goubeaud, R.K. Thauer. *Science*, **278**, 1457 (1997); (b) M. Krüger, A. Meyerdierks, F.O. Glöckner, R. Amann, F. Widdel, M. Kube, R. Reinhardt, J. Kahnt, R. Böcher, R.K. Thauer, S. Shima. *Nature*, **426**, 878 (2003).
[6] (a) L.A. Finney, T.V. O'Halloran. *Science*, **300**, 931 (2003); (b) K.J. Waldron, N. Robinson. *Nat. Rev. Microbiol.*, **7**, 25 (2009).
[7] (a) K.S. Kasprzak, F.W. Sunderman, K. Salnikow. *Mutat. Res.*, **533**, 67 (2003); (b) H. Lu, X. Shi, M. Costa, C. Huang. *Mol. Cell. Biochem.*, **279**, 45 (2005); (c) A. Arita, M. Costa. *Metallomics*, **1**, 222 (2009).
[8] (a) E. Hochuli, W. Bannwarth, H. Dobeli, R. Gentz, D. Stuber. *Biotechnology*, **6**, 1321 (1988); (b) L. Schmitt, C. Dietrich, R. Tampe. *J. Am. Chem. Soc.*, **116**, 8485 (1994); (c) C. Venien-Bryan, F. Balavoine, B. Toussaint, C. Mioskowski, E.A. Hewat, B. Helme, P.M. Vignais. *J. Mol. Biol.*, **274**, 687 (1997); (d) D. Tareste, F. Pincet, M. Brellier, C. Mioskowski, E. Perez. *J. Am. Chem. Soc.*, **127**, 3879 (2005).
[9] (a) E.M. Wilson-Kubalek, R.E. Brown, H. Celia, R.A. Milligan. *Proc. Natl. Acad. Sci. U.S.A.*, **95**, 8040 (1998); (b) N. Bischler, F. Balavoine, P. Milkereit, H. Tschochner, C. Mioskowski, P. Schultz. *Biophys. J.*, **74**, 1522 (1998); (c) L. Lebeau, F. Lach, C. Venien-Bryan, A. Renault, J. Dietrich, T. Jahn, M.G. Palmgren, W. Kuhlbrandt, C. Mioskowski. *J. Mol. Biol.*, **308**, 639 (2001).
[10] (a) S.W. Guo, L. Konopny, R. Popovitz-Biro, H. Cohen, H. Porteanu, E. Lifshitz, M. Lahav. *J. Am. Chem. Soc.*, **121**, 9589 (1999); (b) T.A. Waggoner, J.A. Last, P.G. Kotula, D.Y. Sasaki. *J. Am. Chem. Soc.*, **123**, 496 (2001).
[11] (a) G. Cao, H.G. Hong, T.E. Mallouk. *Acc. Chem. Res.*, **25**, 420 (1992); (b) I.O. Benitez, B. Bujoli, L.J. Camus, C.M. Lee, F. Odobel, D.R. Talham. *J. Am. Chem. Soc.*, **124**, 4363 (2002).
[12] (a) Y.W. Liang, R.H. Schmehl. *J. Chem. Soc., Chem. Commun.*, 1007 (1995); (b) E.C. Constable, W. Meier, C. Nardin, S. Mundwiler. *Chem. Commun.*, 1483 (1999); (c) B.G.G. Lohmeijer, U.S. Schubert. *Angew. Chem., Int. Ed.*, **41**, 3825 (2002).
[13] A. Scheurer, H. Maid, F. Hampel, R.W. Saalfrank, L. Toupet, P. Mosset, R. Puchta, N.J.R. van Eikema Hommes. *Eur. J. Org. Chem.*, 2566 (2005).
[14] (a) K.A. Goldsby. *J. Coord. Chem.*, **19**, 83 (1988); (b) K.A. Goldsby, J.K. Blaho, L.A. Hoferkamp. *Polyhedron*, **8**, 113 (1989).
[15] J.G. Muller, L.A. Kayser, S.J. Paikoff, V. Duarte, N. Tang, R.J. Perez, S.E. Rokita, C.J. Burrows. *Coord. Chem. Rev.*, **185–186**, 761 (1999).
[16] F. Reitzenstein. *Ammoniak, Pyridin-Salze und Hydrate Bivalenter Metalle von gemeinsamen und trennenden Gesichtspunkten*, Habilitationsschrift, Würzburg (1898).
[17] F.A. Cotton, G. Wilkinson. *Advanced Inorganic Chemistry*, 5th Edn, John Wiley & Sons, New York, NY (1988).
[18] (a) D.J. Evans, C. Pickett. *J. Chem. Soc. Rev.*, **32**, 268 (2003); (b) D.J. Evans. *Coord. Chem. Rev.*, **249**, 1582 (2005).
[19] T.C. Harrop and P.K. Mascharak. In *Concepts and Models in Bioinorganic Chemistry*, H.-B. Kraatz and N. Metzler-Nolte (Ed.), p. 309, Wiley-VCH, Weinheim, (2006).
[20] L. Rulíšek, Z. Havlas. *J. Phys. Chem. A*, **103**, 1634 (1999).
[21] P.R. Varadwaj, I. Cukrowski, H.M. Marques. *J. Phys. Chem. A*, **112**, 10657 (2008).
[22] R.K. Hocking, R.J. Deeth, T.W. Hambley. *Inorg. Chem.*, **46**, 8238 (2007).
[23] *Spartan 4.0*, Wavefunction Inc., 18401 Von Karman Ave., 370 Irvine, CA 92715, USA, ©1995 Wavefunction, Inc.
[24] (a) AM1: M.J.S. Dewar, E.G. Zoebisch, E.F. Healy, J.J.P. Stewart. *J. Am. Chem. Soc.*, **107**, 3902 (1985); (b) AM1*: H. Kayi, T. Clark. *J. Mol. Model.*, **16**, 29 (2010).
[25] J.J.P. Stewart. *J. Mol. Model.*, **13**, 1173 (2007).
[26] *Titan*, Wavefunction, Inc. and Schrodinger Inc. 18401 Von Karman Avenue, Suite 370, Irvine, CA 92612, USA.
[27] *VAMP 10.0*, T. Clark, A. Alex, B. Beck, F. Burkhardt, J. Chandrasekhar, P. Gedeck, A. Horn, M. Hutter, B. Martin, G. Rauhut, W. Sauer, T. Schindler, T. Steinke, Erlangen (2003).
[28] (a) A.D. Becke. *J. Phys. Chem.*, **97**, 5648 (1993); (b) C. Lee, W. Yang, R.G. Parr. *Phys. Rev. B*, **37**, 785 (1988); (c) P.J. Stephens, F.J. Devlin, C.F. Chabalowski, M.J. Frisch. *J. Phys. Chem.*, **98**, 11623 (1994); (d) T.H. Dunning Jr, P.J. Hay. Mod. Theor. Chem., **3**, 1 (1976); (e) P.J. Hay, W.R. Wadt. *J. Chem.*

Phys., **82**, 270 (1985); (f) P.J. Hay, W.R. Wadt. *J. Chem. Phys*., **82**, 284 (1985); (g) P.J. Hay, W.R. Wadt. *J. Chem. Phys*., **82**, 299 (1985); (h) S. Huzinaga (Ed.). Gaussian Basis Sets for Molecular Calculations, Elsevier, Amsterdam (1984).

[29] See e.g. (a) S. Klaus, H. Neumann, H. Jiao, A. Jacobi von Wangelin, D. Gördes, D. Strübing, S. Hübner, M. Hately, C. Weckbecker, K. Huthmacher, T. Riermeier, M. Beller. *J. Organomet. Chem*., **689**, 3685 (2004); (b) R.W. Saalfrank, Ch. Deutscher, H. Maid, A.M. Ako, S. Sperner, T. Nakajima, W. Bauer, F. Hampel, B.A. Heß, N.J.R. van Eikema Hommes, R. Puchta, F.W. Heinemann. *Chem. Eur. J*., **10**, 1899 (2004); (c) P. Illner, A. Zahl, R. Puchta, N.J.R. van Eikema Hommes, P. Wasserscheid, R. van Eldik. *J. Organomet. Chem*., **690**, 3567 (2005); (d) M. Galle, R. Puchta, N.J.R. van Eikema Hommes, R. van Eldik. *Z. Phys. Chem*., **220**, 511 (2006); (e) P. Illner, R. Puchta, F.W. Heinemann, R. van Eldik. *Dalton Trans*., 2795 (2009); (f) B.M. Alzoubi, F. Vidali, R. Puchta, C. Dücker-Benfer, A. Felluga, L. Randaccio, G. Tauzher, R. van Eldik. *Dalton Trans*., 2392 (2009); (g) A. Scheurer, R. Puchta, F. Hampel. *J. Coord. Chem*., **63**, 2868 (2010) and literature cited therein.

[30] (a) V. Barone, M. Cossi. *J. Phys. Chem. A*, **102**, 1995 (1998); (b) M. Cossi, N. Rega, G. Scalmani, V. Barone. *J. Comput. Chem*., **24**, 669 (2003).

[31] M.J. Frisch, G.W. Trucks, H.B. Schlegel, G.E. Scuseria, M.A. Robb, J.R. Cheeseman, G. Scalmani, V. Barone, B. Mennucci, G.A. Petersson, H. Nakatsuji, M. Caricato, X. Li, H.P. Hratchian, A.F. Izmaylov, J. Bloino, G. Zheng, J.L. Sonnenberg, M. Hada, M. Ehara, K. Toyota, R. Fukuda, J. Hasegawa, M. Ishida, T. Nakajima, Y. Honda, O. Kitao, H. Nakai, T. Vreven, J.A. Montgomery, Jr., J.E. Peralta, F. Ogliaro, M. Bearpark, J.J. Heyd, E. Brothers, K.N. Kudin, V.N. Staroverov, R. Kobayashi, J. Normand, K. Raghavachari, A. Rendell, J.C. Burant, S.S. Iyengar, J. Tomasi, M. Cossi, N. Rega, J.M. Millam, M. Klene, J.E. Knox, J.B. Cross, V. Bakken, C. Adamo, J. Jaramillo, R. Gomperts, R.E. Stratmann, O. Yazyev, A.J. Austin, R. Cammi, C. Pomelli, J.W. Ochterski, R.L. Martin, K. Morokuma, V.G. Zakrzewski, G.A. Voth, P. Salvador, J.J. Dannenberg, S. Dapprich, A.D. Daniels, O. Farkas, J.B. Foresman, J.V. Ortiz, J. Cioslowski, D.J. Fox. *Gaussian 09*, Revision A.02, Gaussian, Inc., Wallingford CT (2009).

[32] M.J. Frisch, G.W. Trucks, H.B. Schlegel, G.E. Scuseria, M.A. Robb, J.R. Cheeseman, J.A. Montgomery, Jr., T. Vreven, K.N. Kudin, J.C. Burant, J.M. Millam, S.S. Iyengar, J. Tomasi, V. Barone, B. Mennucci, M. Cossi, G. Scalmani, N. Rega, G.A. Petersson, H. Nakatsuji, M. Hada, M. Ehara, K. Toyota, R. Fukuda, J. Hasegawa, M. Ishida, T. Nakajima, Y. Honda, O. Kitao, H. Nakai, M. Klene, X. Li, J.E. Knox, H.P. Hratchian, J.B. Cross, V. Bakken, C. Adamo, J. Jaramillo, R. Gomperts, R.E. Stratmann, O. Yazyev, A.J. Austin, R. Cammi, C. Pomelli, J.W. Ochterski, P.Y. Ayala, K. Morokuma, G.A. Voth, P. Salvador, J.J. Dannenberg, V.G. Zakrzewski, S. Dapprich, A.D. Daniels, M.C. Strain, O. Farkas, D.K. Malick, A.D. Rabuck, K. Raghavachari, J.B. Foresman, J.V. Ortiz, Q. Cui, A.G. Baboul, S. Clifford, J. Cioslowski, B.B. Stefanov, G. Liu, A. Liashenko, P. Piskorz, I. Komaromi, R.L. Martin, D.J. Fox, T. Keith, M.A. Al-Laham, C.Y. Peng, A. Nanayakkara, M. Challacombe, P.M.W. Gill, B. Johnson, W. Chen, M.W. Wong, C. Gonzalez, J.A. Pople. *Gaussian 03*, Revision C.02, Gaussian, Inc., Wallingford, CT (2004).

[33] E. Gyepes, T. Głowiak. *Acta Cryst*., **C45**, 391 (1989).

[34] V.V. Fomenko, T.N. Polynova, M.A. Porai-Koshits. *Zh. Strukt. Khim*., **16**, 651 (1975).

[35] K.-Y. Choi, S.N. Choi, C.P. Hong. *J. Inclusion Phenom. Macrocyclic Chem*., **40**, 67 (2001).

[36] S.R. Choudhury, P. Gamez, A. Robertazzi, C.-Y. Chen, H.M. Lee, S. Mukhopadhyay. *Cryst. Growth Des*., **8**, 3773 (2008).

[37] I.N. Polyakova, T.N. Polynova, M.A. Porai-Koshits. *Koord. Khim*., **8**, 1268 (1982).

[38] I.N. Polyakova, A.L. Poznyak, V.S. Sergienko. *Kristallografiya*, **45**, 833 (2000).

[39] J.R. Harjani, T. Friscic, L.R. MacGillivray, R.D. Singer. *Dalton Trans*, 4595 (2008).

[40] Tetra anions cannot be calculated by Titan.

[41] C_i: NImag = 1, $-5.20\,cm^{-1}$.

[42] C_i: NImag = 1, $-2.95\,cm^{-1}$.

[43] Due to parameter problems, Ni–Se could not be calculated.

[44] Te–Ni: 3.52 Å, therefore not included.

[45] Due to parameter problems, Ni–Te could not be calculated.

[46] Due to parameter problems, Ni–As could not be calculated.

[47] Due to parameter problems, Ni–Sb could not be calculated.

[48] No parameter available.

[49] Te–Ni: 3.80 Å, therefore not included.